



# Lectures notes on Advanced Computational Statistical Physics

## Contents

<b>1 Introduction</b>	<b>1</b>
I Computational Statistical Physics . . . . .	1
II Invariant Measures and Ergodicity . . . . .	1
<b>2 Molecular Dynamics</b>	<b>2</b>
I Hamiltonian Dynamics . . . . .	2
A Hamiltonian Formalism . . . . .	2
B Map Flow . . . . .	2
C Symplectic Form . . . . .	2
D Error Analysis for Hamiltonian splitting	2
II Time Integration . . . . .	3
A Application to the Harmonic Oscillator .	3
<b>3 Constant Temperature Dynamics</b>	<b>5</b>
I Different Ensembles . . . . .	5
A Microcanonical Ensemble . . . . .	5
II Canonical Ensemble . . . . .	5
III Thermostats . . . . .	5
A Stochastic thermmostat Thermostat .	6
B Deterministic Thermostat . . . . .	6
C Comparing Thermostats . . . . .	7
D Calculating Transport Coefficients .	8
<b>4 Metropolis Algorithm</b>	<b>9</b>

## Introduction

In the 19th century, classical mechanics, rooted in Newton's laws, dominated physics. Pierre-Simon Laplace famously articulated the deterministic worldview: given the initial conditions of a system, its future could be perfectly predicted through precise mathematical equations. This perspective treated the universe like a clockwork machine, where every event followed from the initial state.

However, as the study of thermodynamics and many-particle systems advanced, the limits of this purely deterministic approach became clear. Statistical physics emerged to address these complexities, particularly through the work of James Clerk Maxwell and Ludwig Boltzmann. Their pioneering contributions, such as Maxwell's velocity distribution in gases and Boltzmann's statisti-

cal interpretation of entropy, introduced probabilistic methods to understand the behavior of large ensembles of particles.

In this new framework, the precise motion of individual particles became less important; instead, statistical averages and distributions described macroscopic properties like temperature and pressure. While Laplace envisioned a universe governed by strict determinism, statistical physics embraced the unpredictability inherent in large systems, marking a profound shift in understanding.

This shift continued to resonate into the 20th century, influencing the work of physicists like Philip W. Anderson. Anderson famously argued that "more is different," suggesting that the behavior of complex systems cannot be fully understood by analyzing individual components alone. This echoes the insights of 19th-century statistical physics, where collective behavior emerged from many interacting parts, challenging the reductionist views of classical mechanics.

In summary, while classical mechanics remained essential for describing deterministic systems, the development of statistical physics in the 19th century introduced a probabilistic approach that transformed our understanding of many-body systems and laid the groundwork for modern physics.

## I. Computational Statistical Physics

Computational methods allow us to simulate these complex systems directly, providing detailed insights into their behavior. Using modern computing power, scientists can model the interactions of millions, or even billions, of particles, making it possible to observe emergent phenomena such as phase transitions, critical behavior, and chaotic dynamics. This computational approach helps us overcome the "many-body" problem, where the sheer number of interactions in a system defies exact solutions.

One reason computational statistical physics is so powerful is that it can handle systems that are analytically intractable. For instance, systems with strong correlations between particles or those far from equilibrium, which are difficult to study using traditional methods, can be simulated using Monte Carlo techniques, molecular dynamics, and other algorithms.

Additionally, computational approaches enable the study of phenom-

ena at different scales—from the atomic scale, where quantum effects dominate, to macroscopic scales governed by classical statistical physics. This versatility allows for a deeper understanding of both microscopic mechanisms and their macroscopic consequences, bridging the gap between theoretical models and real-world systems.

In essence, computational statistical physics allows us to explore systems that are too complex for exact solutions, providing a practical and powerful way to study emergent behavior, phase transitions, and non-equilibrium systems. By leveraging the power of computers (which is increasing exponentially since the second half of the 19th century Fig. 1.1), it opens up new frontiers for understanding the vast complexity of the physical world, which neither classical mechanics nor early analytical statistical methods could fully address.

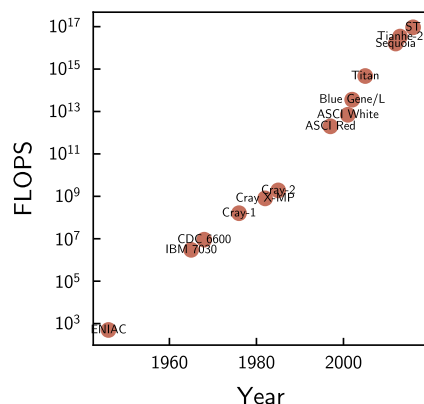


Figure 1.1 – Number of Floating points operations evolution for the biggest supercomputer

## II. Invariant Measures and Ergodicity

In statistical physics, the concept of an invariant measure plays a crucial role in understanding the long-term behavior of dynamical systems, and the symmetry of the system (Noether's theorem). One of the main goals of computational statistical physics is to find algorithms preserving the invariant measure of the systems we are studying. For example we will see that the Euler algorithm is not a good choice for simulating Hamiltonian systems, as it does not conserve the energy of the system, as opposed to the Verlet algorithm, which is based on clever considerations of the symplectic<sup>1</sup> structure of the phase space.

<sup>1</sup>Refers to the Hamiltonian Formulation of classical mechanics



Ergodicity is another important concept in statistical physics, which ensures that the system explores the entire phase space in the long run. Which results in one of the most important hypothesis in computational statistical physics, the ergodic hypothesis, which states that the time average of a system is equal to its ensemble average (limit cases CITE).

## Molecular Dynamics

### I. Hamiltonian Dynamics

#### A. Hamiltonian Formalism

The Legendre transformation of the Lagrangian allows us to define the Hamiltonian of a system, which is a function of the generalized coordinates  $q_i$  and the generalized momenta  $p_i$  of the system (see CITE). The Hamiltonian is defined as :

$$H \stackrel{\text{def}}{=} \frac{\mathbf{p}^T \mathbf{M}^{-1} \mathbf{p}}{2} + U(q)$$

with  $U(q)$  the potential energy of the system and  $\mathbf{M}$  the mass matrix of the system. The equations of motions can then be written using the Euler-Lagrange equations :

$$\begin{cases} \dot{q} = \frac{\partial H}{\partial p} \\ \dot{p} = -\frac{\partial H}{\partial q} \end{cases}$$

This can be written in a more compact matrix form :

$$\begin{pmatrix} \dot{\mathbf{q}} \\ \dot{\mathbf{p}} \end{pmatrix} = \mathbf{J} \nabla H(\mathbf{p}, \mathbf{q})$$

with

$$\mathbf{J} = \begin{pmatrix} 0 & \mathbf{I} \\ \mathbf{I} & 0 \end{pmatrix}$$

These type of non linear equations can only be locally, but since the systems are Hamiltonian we can unearth the global existence and uniqueness of the solutions. Indeed we just need to show that using the energy constraints of the system the solutions are bounded for all time. For the impulsion this is trivial considering a potential global minimum :

$$\frac{\mathbf{p}^T \mathbf{M}^{-1} \mathbf{p}}{2} \leq E_0 - U_{min}$$

for the position we just need an assumption on the level sets of the potential energy.

$$\Sigma_\alpha = \{\mathbf{q} | U(\mathbf{q}) = \alpha\}$$

If these lebel are bounded then the solutions are bounded for all time. This is not the case for all potentials, this is why for solving this kind of equations we will add sometimes confining potentials to the system.

#### B. Map Flow

Since the Hamiltonian equations are solvable, it seems natural to define a map flow  $\mathcal{F}$  such that for an initial condition  $\mathbf{z}_0$  and a considered point  $\mathbf{z}_t$  we have :

$$\mathbf{z}_t = \mathcal{F}_t(\mathbf{z}_0)$$

This flow map is obviously invertible and Hamiltonian conservative. The key of numerical integration is then to approximate the true flow map of the system by the numerical flow map  $\mathcal{T}$  such that the physical properties of the system are conserved over time.

Considering the linear system for the differentiation :

$$\frac{d\mathbf{z}}{dt} = f(\mathbf{z}) = A\mathbf{z} \quad (2.1)$$

One way to solve this equation is to use the matrix exponential :

$$\mathbf{z}_t = \exp(At)\mathbf{z}_0$$

Then it appears that the flow map is given by :

$$\mathcal{F}_t(\mathbf{z}) = \exp(tA)\mathbf{z} \quad (2.2)$$

#### C. Symplectic Form

##### a) Volume Preservation

One of the most important properties of the flow map is the preservation of the volume in the phase space. Indeed, for a Hamiltonian system we have thanks to Liouville's theorem the volume of a given sets of solution governed by Eq. (2.1) is preserved over time if

$$\nabla \cdot f = 0.$$

It is easy to show that for a Hamiltonian system :

$$\nabla \cdot f = \nabla \cdot \begin{pmatrix} 0 & \mathbf{I} \\ \mathbf{I} & 0 \end{pmatrix} \nabla H = 0$$

Due to the  $\mathcal{C}^2$  property of the Hamiltonian. The main consequence of this property is that the flow map is volume preserving, which has to be an important property of the integration algorithm to approximate the flow map.

Volume preservation is a key property since it ensures that the numerical integration keeps the hamiltonian structure of the system, following the liouville theorem i.e the conservation of the phase space volume along particles trajectories in the phase space.

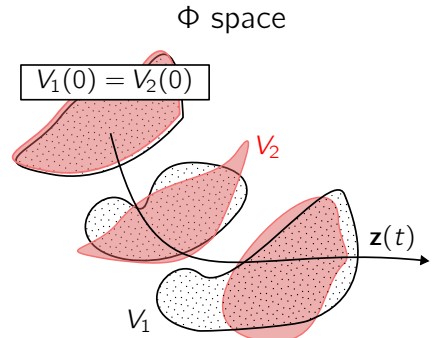


Figure 2.1 – Volume conservation for the true Hamiltonian in black and the approximated Hamiltonian in red

##### b) Symplectic Property

The symplectic property of the flow map is another important property of the Hamiltonian system. Indeed, the symplectic property of the flow map is defined as :

$$\mathcal{F}_t^T J \mathcal{F}_t = J$$

With  $J = \begin{pmatrix} 0 & \mathbf{I} \\ -\mathbf{I} & 0 \end{pmatrix}$  the symplectic matrix. This property leads to the conservation of the volume of the phase space, indeed we have for the jacobian associated with the map :  $|\mathcal{F}'_t|^2 = 1$ .

One interesting point of symplectic maps is that they form a group (they preserved the composition) which can be used to build other more complex symplectic maps. For example to increase the order of symplectic integrators  $\mathcal{G}_h$  approximating the flow map  $\mathcal{F}_h$ , we can also split wut Hamiltonian just dependant of the impulsion or the position. This is called the splitting method, which is based on the Trotter expansion of the flow map (Find symplectic form of splitted hamiltonian).

#### D. Error Analysis for Hamiltonian splitting

##### a) Lie Derivatives and Poisson Brackets

###### Lie Derivatives

In the case of a non-Linear Hamiltonian system, the flow map can be approximated by the Lie derivative of the Hamiltonian, we would like to find again the convenient results :

$$\mathcal{F}_t = \exp(tA)\mathbf{z}$$

Let's consider a functional  $\Phi$  of the phase space, the Lie derivative of  $\Phi$  is defined as :

$$\mathcal{L}_f \Phi = \nabla \Phi \cdot f$$



This is a generalization of the directional derivative to the phase space. Expanding the  $\Phi$  map in a Taylor series we have :

$$\begin{aligned}\Phi(\mathbf{z}(t)) &= \sum_i \frac{t^i}{i!} (\mathcal{L}_f^i \Phi)(\Phi(\mathbf{0})) \\ &= \exp(t\mathcal{L}_f)(\Phi(\mathbf{0}))\end{aligned}$$

Applying this along the trajectory gives us the following map :

$$\mathcal{F}_t(\mathbf{z}) = \exp(t\mathcal{L}_f)(\mathbf{z})$$

As we wanted.

### Poisson Brackets

A common notation introduced in Hamiltonian mechanics is the Poisson bracket, which is defined as :

$$\begin{aligned}\{g_1, g_2\} &= \sum_{i=1}^N \left( \frac{\partial g_1}{\partial q_i} \frac{\partial g_2}{\partial p_i} - \frac{\partial g_2}{\partial q_i} \frac{\partial g_1}{\partial p_i} \right) \\ &= \nabla g_1^T \mathbf{J} \nabla g_2\end{aligned}$$

Considering a smooth scalar value function  $F$  of the phase space, we can show that the Lie derivative of  $F$  is given by the Poisson bracket of  $F$  and the Hamiltonian :

$$\mathcal{L}_{\mathbf{J} \nabla H} F = \mathcal{L}_H F = \{F, H\}$$

Poisson brackets can be related to the Lie deriving noticing that for every real valued function  $f$ :

$$[\mathcal{L}_{H_1}, \mathcal{L}_{H_2}]f = \mathcal{L}_{\{H_1, H_2\}}f$$

### b) Error Analysis for non Commuting Hamiltonian

The main idea behinds this study is to consider integration method as a splitting of the Hamiltonian into several parts oftenly independant of one of the two system of coordinates  $(\mathbf{q}, \mathbf{p})$ , as we will see further. The poisson brackets are linear with respect to the Hamiltonian, which allows us to write the following considering  $H = H_1 + H_2$ ,

$$\mathcal{L}_H = \mathcal{L}_{H_1} + \mathcal{L}_{H_2}$$

The flow map of the system is then defined as :  $\mathcal{F}_t(\mathbf{z}) = e^{t(\mathcal{L}_{H_1} + \mathcal{L}_{H_2})} \mathbf{z}$

The splitting method has the following flow map :

$$\mathcal{G}_t h = e^{t\mathcal{L}_{H_1}} e^{t\mathcal{L}_{H_2}}$$

Which is not the same as the true flow map. To evaluate the error done considering the splitted Hamiltonian, we can use the Baker-Campbell-Hausdorff formula [CITE] and the correspondance between the Lie derivative and the Poisson bracket unearthing :

$$e^{t\mathcal{L}_{H_1}} e^{t\mathcal{L}_{H_2}} = e^{t\mathcal{L}_{\tilde{H}_h}}$$

With  $\tilde{H}_h$  the shadow Hamiltonian :

$$\begin{aligned}\tilde{H}_h &= H_1 + H_2 + \frac{h}{2} \{H_1, H_2\} + \\ &\quad \frac{h^2}{12} (\{H_1 \{H_1, H_2\}\} - \{H_2 \{H_1, H_2\}\}) \dots\end{aligned}$$

From this we can easily understand that as long as the two splitted Hamiltonian do not commute, we have at least an linear error (on example is the symplectic Euler Method). One way to do that, is to find a split with commutating hamiltonian, or to split  $H$  into three hamiltonian such that that the linear term vanishes (such as the Velvet velocity & position method). The main idea behind this development was to show that the flow map  $\mathcal{F}_t$  we approximate using the other  $\mathcal{G}_t$  stands in the splitting method for an exact solution to a other (but similar) hamiltonian system.

To put in a nutshell the splitting method allows us to build sympletic integrator using Hamiltonian transformations. Not all intersteing integrators have sympletic structures, but they should all conserve volume in the phase space.

## II. Time Integration

Here we will restrict our study to linear system. To perform time integration, we discretize time into small intervals  $\delta t$ . At each time step  $t_{n+1} = n\delta t$ , we approximate the change in the system using matrix iteration.

$$\begin{pmatrix} x(n\delta t) \\ y(n\delta t) \end{pmatrix} = \mathcal{T}^n(\delta t) \begin{pmatrix} x(0) \\ y(0) \end{pmatrix}$$

The goal is then to find the correct matrix such that iterating over time will not change the invariance of the system. To fit the previous notations the flow map can be defined as :

$$\mathcal{F}_{\delta t}(\mathbf{z}) = \mathcal{T}(\delta t)\mathbf{z}$$

with  $\mathcal{F}_{\delta t}$  a volume conservative flow map.

### A. Application to the Harmonic Oscillator

$$\ddot{x} - \omega^2 x = 0$$

#### a) Exact Propagator

For the harmonic oscillator, the time evolution is well known which is useful to test the time integration algorithms. Indeed, we got :

$$\begin{pmatrix} x(\delta t) \\ \dot{x}(\delta t) \end{pmatrix} = \mathcal{T}(\delta t) \begin{pmatrix} x(0) \\ \dot{x}(0) \end{pmatrix}$$

With

$$\mathcal{T}(\delta t) = \begin{pmatrix} \cos(\omega t) & \frac{1}{\omega} \sin(\omega t) \\ \omega \sin(\omega t) & \cos(\omega t) \end{pmatrix}$$

In the next analysis we will use a dimensionless time  $\tau = \omega t$ , a dimensionless position  $\xi = \sqrt{\frac{k}{k_B T}} x$  and a dimensionless impulsion  $\Pi = \sqrt{\frac{1}{m k_B T}} p$ , which leads to the following time Propagator :

$$\begin{aligned}\mathcal{F}_{\delta \tau} &= \mathcal{T}(\delta \tau) = \begin{pmatrix} \cos(\delta \tau) & \sin(\delta \tau) \\ -\sin(\delta \tau) & \cos(\delta \tau) \end{pmatrix} \\ &= \exp(\mathbf{J} \tau)\end{aligned}$$

Here we related as did previously the flow map to the derivative operation for our system. For the Hamiltonian we find :

$$H = \frac{\mathcal{H}}{k_B T} = \frac{1}{2} (\Pi^2 + \xi^2)$$

Then let's consider a microstate of the system  $|\tau\rangle = \begin{pmatrix} \xi(\tau) \\ \Pi(\tau) \end{pmatrix}$  The time evolution of the system is given by the following equation :

$$|\tau + \delta \tau\rangle = \mathcal{T}(\delta \tau)|\tau\rangle$$

With the unitary propagation matrix

$$\mathcal{T}(\delta \tau) = \begin{pmatrix} \cos(\delta \tau) & \frac{1}{\omega} \sin(\delta \tau) \\ -\omega \sin(\delta \tau) & \cos(\delta \tau) \end{pmatrix}$$

Solving the characteristic equation  $\|\mathcal{T} - \lambda I\| = 0$ , we unearth the eigenvalues.

$$\lambda_{\pm} = \exp(\pm i \delta \tau),$$

Considering the two orthogonal eigenvectors  $|\pm\rangle$ , we easily show that :

$$\begin{aligned}|n\delta t\rangle &= \mathcal{T}(\delta t)^n |0\rangle \\ &= a_+ \lambda_+^n |+\rangle + a_- \lambda_-^n |-\rangle\end{aligned}$$

Considering the initial decomposition

$$|0\rangle = a_+ |+\rangle + a_- |-\rangle$$

Then we can easily show that :



$$\begin{aligned}\frac{E}{k_b T} &= \frac{1}{2} \langle n\delta\tau | n\delta\tau \rangle \\ &= \frac{1}{2} (|a_+|^2 |a_-|^2) \mathcal{T}(\delta\tau)^n \\ &= \frac{1}{2} \langle 0|0\rangle\end{aligned}$$

Which shows that the energy is conserved over time. We can also show an interesting result about the conserved quantities :

$$\begin{aligned}\langle 0|A|0\rangle &= \langle \tau|A|\tau\rangle \\ \Rightarrow A &\equiv \mathcal{T}^\dagger A \mathcal{T} \\ \Rightarrow A &\propto H\end{aligned}$$

### b) Euler Algorithm & Propagator

The Euler algorithm is the simplest algorithm to perform time integration, based on the first order approximation in Taylor expansion. The explicit non symplectic Euler algorithm is given by the following flow map :

$$G_{\delta\tau}^{\text{euler}} = I - S\delta\tau$$

With  $S$  verifying

$$\frac{dz}{d\tau} = Sz$$

One can remark that for volume conservation the map should verify the following property :

$$\det(I - S\delta\tau) = 0$$

, which is generally not the case in physical system were the eigen values of  $S$  are oftenly pure imaginary. If we write the propagation matrix for the Euler algorithm, we obtain the following :

$$\mathcal{T}(\delta\tau) = \begin{pmatrix} 1 & \delta\tau \\ -\omega^2\delta\tau & 1 \end{pmatrix}$$

Which is not unitary, and not time reversible. We can show that the energy of the system is not conserved over time, through the same reasoning as before. The two eigenvalues of the matrix are :

$$\lambda_\pm = 1 \pm i\delta\tau$$

Which leads to divergence of the energy with the following expression :

$$\begin{aligned}H &= \frac{1}{2} \langle 0|0\rangle (1 + \delta\tau^2)^n \\ &= \frac{1}{2} \langle 0|0\rangle \exp(n \ln(1 + \delta\tau^2))\end{aligned}$$

This divergence of the system can be seen in the following figure

### c) Verlet Algorithm & Propagator

The Verlet algorithm is a second-order algorithm, which is based on the symplectic structure of the phase space and directly derived from the splitting method. The point is to split the Hamiltonian into two parts, one depending only on the position and the other only on the impulsion.

$$H = H_q + H_p$$

With  $H_q = U(q)$  and  $H(p) = \frac{p^T M^{-1} p}{2}$ . If we just do that it is obviously from the shadow Expansion of the Hamiltonian (REF EQ) an order one method (the Euler symplectic method). For the velvet algorithm we want that the order one term vanishes in, which leads to the following splits:

$$H = H_1 + H_2 + H_3$$

with the following possibility :

$$\begin{cases} H_1 = H_3 = \frac{1}{4} p^T M^{-1} p & | \quad H_2 = U(q) \\ H_1 = H_3 = \frac{1}{2} U(q) & | \quad H_2 = \frac{1}{2} p^T M^{-1} p \end{cases}$$

One can show that the first oder term vanishes in the shadow Hamiltonian, which defined a second order method. The first split is called the **position Verlet algorithm**, and the second the **velocity Verlet algorithm**. Let's focus on the velocity algorithm, this split is equivalent to the following change of variable :

$$\hat{\mathbf{P}} = \mathbf{P} - \frac{h}{2} \nabla U(\mathbf{q}) \quad (2.3)$$

$$\mathbf{Q} = \mathbf{q} + \frac{h}{2} \mathbf{p}^T M^{-1} \mathbf{p} \quad (2.4)$$

$$\mathbf{P} = \hat{\mathbf{P}} - \frac{h}{2} \nabla U(\mathbf{Q}) \quad (2.5)$$

This consist in a first drift  $\frac{h}{2} \nabla U(\mathbf{q})$ , following by a kick  $\frac{h}{2} \mathbf{p}^T M^{-1} \mathbf{p}$  and a final kick. This respect the hamiltonian stucture of the system and gives the following propagation matrix :

$$\mathcal{T}(\delta\tau) = \begin{pmatrix} 1 - \frac{\delta\tau^2}{2} & \delta\tau \\ -\delta\tau \left(1 - \frac{1}{4}\delta\tau^2\right) & 1 - \frac{\delta\tau^2}{2} \end{pmatrix}$$

Here we find an unitary matrix, which conserves the pseudo energy of the system over time. Indeed using this scheme the eigenspaces are not orthogonal anymore, the true energy is then not conserved however we can still study the conserved quantities and show that :

$$\begin{aligned}\langle 0|A|0\rangle &= \langle \tau|A|\tau\rangle \\ \Rightarrow A &\equiv \mathcal{T}^\dagger A \mathcal{T} \\ \Rightarrow A &\propto \begin{pmatrix} 1 & 0 \\ 0 & \frac{1}{(1-\delta\tau^2/2)^2} \end{pmatrix} \xrightarrow{\delta\tau \rightarrow 0} H\end{aligned}$$

This can be related to the discussion on the *shadow* Hamiltonian, were we saw that the Hamiltonian describing the system in these kind of integrations was changing, due to commutator terms. Hence, the true energy is not conserved but the energy corresponding to the exact description of the integration system is definitely conserved.

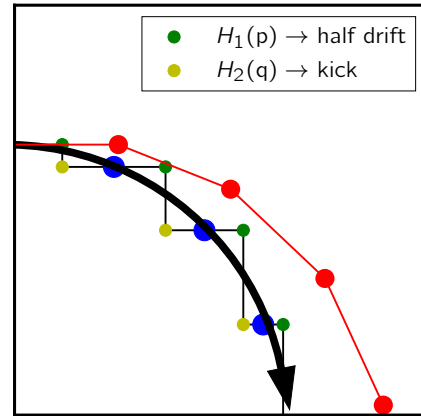
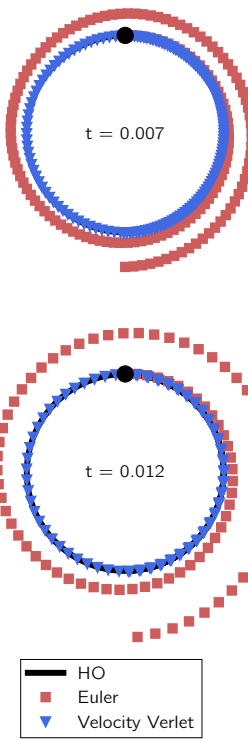


Figure 2.2 – Here we compared the construction of the flow map for the euler and the velvet algorithm. We can see that for great time steps the Euler algorithm diverges from the true flow map, while the velvet algorithm stays close to the true flow map.

This is quite relevant to notice that for periodic system the euler algorithm is definitely not stable due to the non conservation of the volume. We can also see that as a consequence of taking the tangent for each time steps as the true flow map, since it will leads us further from the trajectory in the phase space at each time step. This is why the velvet algorithm is a better choice for time integration of Hamiltonian systems.



**Figure 2.3 –** To have a more general view of the efficiency of the integration scheme using a simple Harmonic oscillator we plotted the phase space trajectories for the Euler and the Velvet Algorithm, for two different timestep values

scopic components. The concept of ensembles is fundamental in statistical mechanics because it allows the connection between microscopic interactions (the behavior of individual particles) and macroscopic observables (such as temperature, pressure, and magnetization).

### A. Microcanonical Ensemble

The microcanonical set is the simplest ensemble in statistical mechanics, where the system is isolated and has a fixed energy. It is described using a constant number of particles  $N$ , volume  $V$ , and energy  $E$ . In an isolated system the fundamental postulates states that the system will explore all possible microstates with the same probability. Hence we can define the density of micro-states for the microcanonical ensemble as :

$$\rho_{\text{eq}} = \frac{1}{\Omega}$$

Where  $\Omega$  is the number of microstates of the system with energy  $E$ , some key properties can be derived from this definition, such as the entropy of perfect gas, thermodynamic equilibrium pressure and chemical potential properties, but we will assume that known for the reader. The Microcanonical ensemble is the one used when one simulate a physical system due to conservation laws regarding the Energy, however it is much more convenient to work with constant Temperature, for this we can introduce the canonical ensemble.

### II. Canonical Ensemble

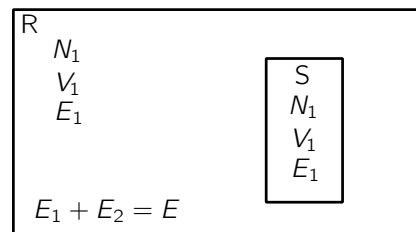


**Figure 3.1 –** Canonical ensemble schematic representation

In the Canonical ensemble we consider that our system is in contact with a big reservoir, thus this two system composed a bigger isolated system. Then since the system  $\mathcal{S} + \mathcal{R}$  is a microcanonical ensemble we get the following :

$$\rho_S = \frac{\Omega_{\mathcal{R}}(E_{\mathcal{R}} = E - E_S)}{\Omega_{\text{tot}}}$$

Considering the reservoir at equilibrium we get :

$$\Omega_{\mathcal{R}}(E_{\mathcal{R}} = E - E_S) = \exp \left[ \frac{S_R}{k_B}(E - E_S) \right]$$

then if we develop the entropy around the mean energy of the system we get :

$$\rho_S = \frac{1}{Z} \exp \left( -\frac{E_S}{k_B T_0} \right)$$

This stands for the Boltzmann-Gibbs distribution with  $Z$  defining the partition function of the canonical ensemble and verifying the following relation :

$$Z = \sum_n \exp(-E_n/k_B T_0)$$

A simple formulation of the partition function can be derived counting the degeneracy of the Energy level  $\omega = e^{S(\epsilon)/k_B}$ . This will lead to the following expression :

$$Z = \int \exp(-\beta(E - T_0 S(E))) dE \quad (3.1)$$

This motivates the definition of the free energy  $F = E - TS$ , and developing this latter around its minimum at the second order in the integrand gives the following :

$$Z = e^{-\beta(E^* - T_0 S(E^*))} \sqrt{\frac{2\pi k_B}{-\frac{\partial^2 S(E^*)}{\partial E^2}}} \quad (3.2)$$

This can be used to prove that the free energy is minimal at equilibrium in the thermodynamic limit. But here we will show that this imply a gaussian distribution of the energy. Indeed using the previous calculation is leads to :

$$p(E) \propto e^{\frac{(E-E^*)^2}{2k_B T_0^2}} \frac{\partial^2 S(E^*)}{\partial E^2}$$

The study of the second moment then unearth :

$$\langle \Delta E^2 \rangle = -k_B \frac{\partial^2 S(E^*)}{\partial E^2} = k_B T_0^2 C_V \quad (3.3)$$

With  $C_V = \frac{\partial E}{\partial T}_{(e, N, V)}$  the heat capacity at fixed volume. This implied that the considering this latter at constant in a small range of temperature the energy distribution is a gaussian whose width is proportional to  $T^2$ .

### III. Thermostats

This huge reservoir we used in the canonical ensemble is called a thermostat and is really convenient to dissipate

### I. Different Ensembles

In statistical physics, an ensemble is a large collection of hypothetical copies of a system, each representing a possible state that the system can be in. Ensembles are used to describe the macroscopic properties of systems based on the statistical behavior of their micro-



external constraints apply on our system  $S$  while conserving a velocity in rough correspondance with temperature. This reservoir has to be able to exert forces and absorb energy from the system, this interaction can be defined in several ways from deterministic to stochastic method.

### A. Stochastic thermostat Thermostat

#### a) Andersen Thermostat

The Andersen thermostat consists in refreshing the velocities of particles with a given probability at each timestep which  $P = v\delta t$  with the collision rate  $v$ . The refresh process is done by drawing a new velocity from the Boltzmann distribution at the given temperature, this can be done from scrambling or for every particles. This method is really simple and do not introduce concerns about ergodicity. However, despite the equation of motion being unchanged too high collision rate can dominate the underlying dynamics, slowing down the speed of exploring the phase space, and breaking the dynamics. Indeed it will leads to loss of memory and exponential decay of autocorrelation functions, while it is not the case in many MD systems.

In order to tackle this issue Andersen proposed  $v \propto C_T \rho^{\frac{2}{3}} N^{-\frac{2}{3}}$  as a typical collision rate such that it should preserve the dynamics in most cases.

#### b) Langevin Thermostat

Changing the dynamics of the system

The Langevin thermostat is a stochastic thermostat that introduces a friction term and a random force to the modified equations of motion. This thermostat mimics the effect of solvent particles collisions on the particles of the system (like the **Anderson** thermostat). The random force is a gaussian force whose amplitude is chosen independantly from the dynamics but only on the Temperature of the system and the friction coefficient, so the more we damp the system the more we have to excite it, this ensure that eventough we increase the damping effect the exploration of the phase space will not be too slow despite we broke the dynamics (as for the Andersen thermostat), on the other hand if we decrease the damping the exploration of the canonical distribution o energy will be djsajidslower. The position Langevin equatiions in an harmonic potential in stationary state are given by :

$$\begin{cases} 0 = \xi v(t) - kx(t) + f(t) \\ \langle f(t)f(t') \rangle = A\delta(t-t') \\ \langle f(t) \rangle = 0 \end{cases}$$

With the characteristic time  $\tau = \xi/k$

and the friction coefficient  $\xi$ . The solution can be written as following :

$$x(t) = x_0 e^{-t/\tau} + \tau^{-1} \int_0^t e^{-(t-t')/\tau} f(t') dt'$$

#### Amplitude of the noise

And one can easily assert what we previously saw regarding the independance of the random force with the dynamics.

$$\begin{aligned} \langle x(t)^2 \rangle &= A\xi^{-2} \int_{-\infty}^t e^{-2(t-t')/\tau} \\ &= A\xi^{-2} \frac{\tau}{2} = \frac{k_B T}{k} \end{aligned}$$

We then got the following :  $A = 2\xi k_B T$ , this is a pretty interesting results since the noise amplitude is directly proportionnal to the friction constant (the more we damped the more we excite).

#### Mean Square Displacement

At very short time the  $t$  the mean square displacement (**msd**)  $\langle \delta r^2 \rangle$  is only given by inertial effects (expendig at the first order) and using the equipartition theorem on the Kinetic energy,

$$\langle \delta r^2 \rangle = d \frac{k_B T}{m} t^2$$

For longer timescales we have to study the effect of the friction term :

$$\begin{aligned} \langle (x_t - x_0) \rangle^2 &= 2(\langle x^2 \rangle - \langle x_t x_0 \rangle), \\ &= 2 \frac{k_B T}{\tau} (1 - e^{-t/\tau}) \end{aligned}$$

this is done using the equipartition theorem and :

$$\langle x_t x_0 \rangle = 2 \frac{k_B T}{\tau} e^{-t/\tau}$$

For time  $t \ll \tau$  this leads to a diffusive process recovering the Einstein reletation with the diffusion constant :  $D = \frac{k_B T}{\xi}$ ,

$$\langle (x_t - x_0) \rangle^2 = 2Dt$$

The  $\tau$  constant is oftenly several order of magnitude above the characteristic time of the dynamics [CITE]. So we will generally considerate only the inertial and the diffusive regime

$$D = \frac{1}{2} \lim_{t \rightarrow \infty} \frac{d\delta r^2}{dt} \quad (3.4)$$

$$D = \frac{\delta r^2}{2t} \quad (3.5)$$

One can note that the memory loss using the Langevin thermostat will be continuously impacted by the white noise, we used for sampling the canonical ensemble, leading to corrupted autocorrelation functions. To deal with that one can implement an memory term in the noise [CITE], which has to be choosen carfully to not break the dynamics of the system. In addition this stochasticity break the continous behavior of the system, and leads to discontinuity in average variables.

### B. Deterministic Thermostat

Studying the stochastics thermostats leads obviously to find and tweaks all the parameters such that we can preserve the physical behaviour of the system, one can argue that we can use deterministic method to do the same sampling of the canonical ensemble, however these kind of methods generally lacks of ergodicity, and harly reproduce the typical variation of the Kinetic Energy in the canonical ensemble [CITE].

#### a) Velocity Rescaling

The simplest way to obtain a constant temperaure dynamics is to rescale the velocity by a factor :

$$v' = \sqrt{\frac{K}{\mathcal{K}}} v \quad (3.6)$$

With  $K, \mathcal{K}$  respectively the total Kinetic energy and the desired Kinetic energy derived from the targeted temperature. Evans and Morriss (1983b) have shown that it leads to the following ensemble distribubution  $p(\mathbf{r}, \mathbf{q})$ :

$$\delta(K(\mathbf{p}) - K_0) \delta(\mathbf{P} - \mathbf{P}_0) \exp\left(\frac{-V(\mathbf{r})}{k_B T}\right) \quad (3.7)$$

With  $\mathbf{P}, K$  respectively the total momentum and kintetic energy. For the conformation propability distribution it is clearly the canoncial one. For the momentum one (SEE) it does not fit the canoncial distribution. Which can lead to smaller oscillation in kinetic energy than the ones in the canonical ensemble. One can propose to add a specific timescale to relax the normalizationn which defines the Berendsen thermostat, where the velocity is this time slowing rescaled to the desired value :

$$\mathbf{v}' = \mathbf{v} \sqrt{1 + \frac{\delta t}{\tau} \left( \frac{K}{\mathcal{K}} - 1 \right)} \quad (3.8)$$

With  $\tau$  the relaxation time, this method is really simple and can be used for equilibration, however it is not time reversible, and one can also show [CITE]



so rescaling the velocity seems a too strong constraint to sample correctly the canonical ensemble. On average, this will lead to the same results as canonical sampling since every ensemble is, in the thermodynamic limit, equivalents, however for fluctuations dependant observable this will exhibit wrong results. These concerns were of strong interest in the 80's, leading to several (partial) solution.

One way to solve this is to introduce a random velocity rescaling to mimic the fluctuations in the canonical ensemble, this can be done using the simple (3.6) rescaling or the Berendsen rescaling (3.8). To do so we just use a random pick for the Kinetic Energy drawn from the canonical distribution.

$$v' = \sqrt{\frac{\bar{K}}{K}}, \quad \bar{K} \in$$

This is called **Canonical Velocity rescaling** (CVR), and as shown by (Bussi), under the assumption of ergodicity this sample correctly the canonical ensemble. One can argue that the dynamics can be altered, because of this stochasticity.

A other totally deterministic approach is the Nose-Hoover formulation of the Dynamics.

### b) Nose-Hoover Thermostat

The main idea here is to extend the system using two a new coordinate  $s$  and a momentum  $p_s$  representing the reservoir, the energy is then allowed to flow between the system and the reservoir. This leads to the following hamiltonian of the total system :

$$\mathcal{H} = H(\mathbf{p}, \mathbf{r}) + \frac{p_s^2}{2Q} + gk_B T$$

With  $Q$  the thermal inertia of the reservoir,  $g$  the number of degree of freedom of the system. The choices of these parameter must me carefully done in order to ensure close coupling between thermostating and dynamics. The ensemble distribution is then :

$$\exp\left(\frac{-H(\mathbf{q}, \mathbf{p})}{k_B T}\right) \exp\left(\frac{-p_s^2}{2Qk_B T}\right)$$

This beautifully stands for the canonical distribution in  $\mathbf{q}, \mathbf{p}$ . However Nosehimself found that this approach was difficultly exploring the phase for very simple system such as harmonic oscillator. Indeed, Nothing to drive the drive the fluctuations of  $p_s$  [CITE] and fluctuations of the thermostating velocities are necessary to ensure the ergodicity of the system, since it will fill difficulty the phase space (coupling between the system and

the reservoir). One possible solution is nose-hoover thermostatic chains, in order to drive the thermostat velocities with other reservoirs, this stands with the **CVR** as a perfect solution but Bussi argued we lost the beauty and the simplicity of the theory multiplying the thermostatic chain.

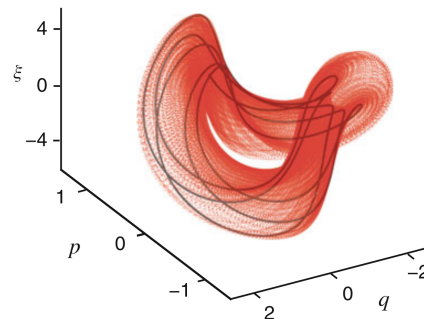


*Figure 3.2 – length 2 Nose Hoover Chain applied on harmoic oscillator, trajectories are caught in an attractor, we do not recover the canonical ensemble distribution (increase the number of chains [CITE], from [CITE])*

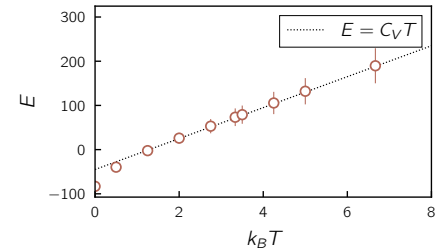


*Figure 3.3 – Energy over Temperature, this plot unearths a value of Heat capacity at fixed volume :  $C_V = 3.5e^1 \pm 1$*

Knowing that we can estimate the canonical distribution of the energy at second order using our previous study (3.3).

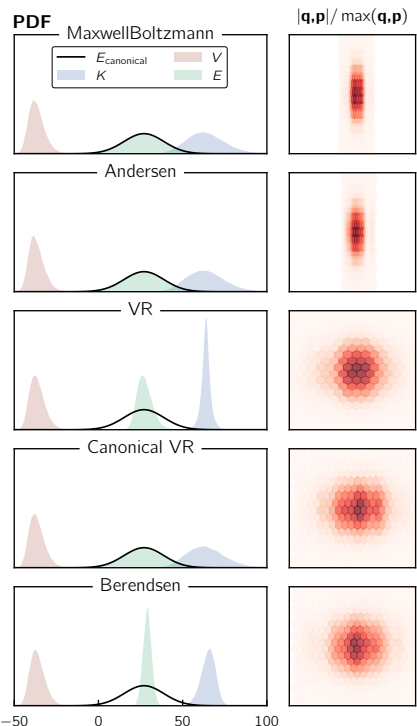


*Figure 3.4 – On the left we plots PDFs of potential  $V$ , kinetic  $K$  and total energy  $E$  for several thermostats. On the right we plot the normalized phase space hexbin histogram (in the sens of explored domain size)*

### C. Comparing Thermostats

Several studies can be done to compare the thermostat, the probability distribution function of the energy to see if it matches the canonical one, with high level of fluctuation. Regarding the dynamics we have to see if the velocity autocorrelation function is not dominated by thermostating effect, leading to corrupted transport coefficient calculation.

#### a) Energy Distribution

Using (3.3) we unearthed that the typical fluctuations of the energy in the canonical ensemble should be quite important, proportional to  $T^2$ . To check which thermostat was able to mimic these fluctuations, we simulated a simple LJ-fluids with 32 particles equilibrated by different thermostats. The first step of the study was to calculate  $C_V$  for this system, to do so we use the **CVR**, and showed that the heat capacity was remaining constant in the range of study.

As intended the **Maxwell Boltzmann**, **Andersen**, **CVR** sample correctly the canonica distribution of energy, which appears normal consideratig their stochastic behavior. For the **VR**, **Berendsen** thermostat their non-canonical properties are clearly demonstrated with very small fluctuations of the Kinetic energy. However, one can notice on the fig 3.4 that the phase space exploration is unefficient for the



**Maxwell-Boltzmann, Andersen** thermostat, with a very restricted exploration of the conformation space, this is mainly due to the fact that we broke the system dynamic, thermostating the velocities too often for this kind of thermostat. This issue does not appear in the three other thermostats, where the phase space exploration is efficient.

To put it in a nutshell thermostating is a subtle problem where we have to find the right equilibrium between sampling correctly the ensemble we want and the phase space in a reasonable time without breaking the dynamics, and ensuring ergodicity.

#### D. Calculating Transport Coefficients

To check if the thermostats preserve the physics of the system, we can study auto-correlation functions. Indeed referring to (Haile and Gupta, 1983), suitable thermostats should preserve the auto-correlation function of the velocity. It is simply a way of checking if the characteristic times of the system are unchanged. In addition to that a whole theory is dedicated to recover transport coefficient from auto-correlation functions (Green-Kubo relations). Here we will focus on the diffusion constant, which can be calculated from the velocity autocorrelation function (VACF).

##### a) Long time tails

In our simulated LJ-system the auto-correlation function of the system should decay slowly at large times, this is called long time tails phenomenon and is universal in this kind of fluid system. The first apparition of this result in the scientific litterature was back in the 70's with the work of Alder and Wainwright simulating hard sphere. Indeed they unearthed a long time tail of the form  $\sim t^{-\frac{d}{2}}$  contradicting the believed exponential decay of autocorrelation function (If we suppose that the dynamic follows the Langevin equation it is quite straightforward that it is the case). This dependency was studied afterward by Pomeau and Résibois using long times hydrodynamics arguments.

The main idea is to rely on the local equilibrium implied by the presence of multiple particles fig.3.5.b) these latter will interact between each other, leading to a constant velocity in a small volume  $\Omega_t$  around the particle of interest, if you consider  $n$  particles interacting in this small volume then :

$$v(\tau) = v(0)/n\Omega_t$$

This volume will spread with time fig.3.5.c) dominated by hydrodynamic

long time viscosity effect :

$$\Omega_t = (\nu t)^{\frac{d}{2}}$$

with  $d$  the dimensionality of the system. This leads to the following expression for the velocity autocorrelation function :

$$v(\tau) \sim v(0) \left( \frac{1}{\nu t} \right)^{\frac{d}{2}} \quad (3.9)$$

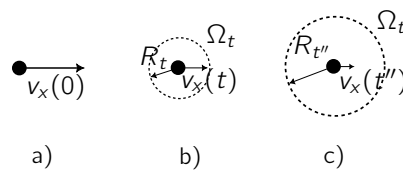


Figure 3.5 – Schematics picturing the slow decay of autocorrelation functions, redrawn from (Pomeau, Resibois)

This dissipative spreading of the small volume  $\Omega_t$  can be pictured by the following reasoning : considering a particle interacting in a repulsive way with other particles, this interaction will create an eddy behind the particle that will ensure that the particle continues in its original direction during a sufficiently long time.

##### Memory loss

This slow memory loss is a key feature of the system, and can be used to check if the dynamics of the system is preserved by the thermostat. Indeed if the thermostat is too strong, the long time tail will be altered.

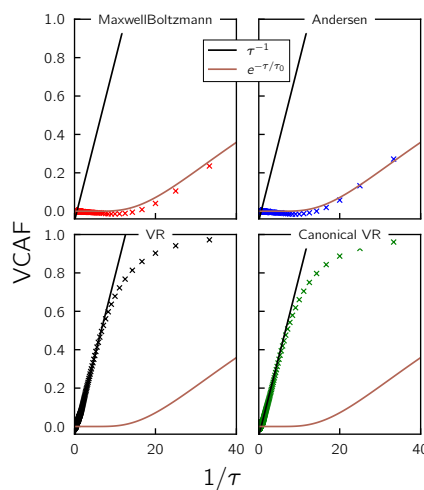


Figure 3.6 – Normalized Velocity autocorrelation function

##### Dependence of the density

To fall in this regime the system has to be dense enough as highlighted by [CITE]. Indeed the long time tail is a collective effect, and will be more pronounced in dense systems, where the particles are more likely to interact with each other and the vortex formation may not be sustained. To check this behavior we simulated the same 2d system. Since the regime we studies should be dominated by collisions, we must know the time between the collision, the Enskog kinetic theory predicts :

$$\tau_E = \frac{1}{4\rho\sigma^2 g(\sigma)} \sqrt{\frac{m}{\pi k_B T}} \quad (3.10)$$

With  $g(\sigma)$  the radial distribution function at the contact distance  $\sigma$ , this will be the characteristic length of the LJ potential in our case. For hard spheres it gives the following [CITE] :

$$g(\sigma) = \frac{1 - \pi\sigma^3\rho/12}{(1 - \pi\sigma^3\rho/6)^3}$$

We then decided to normalize the time by this time, and plot the VACF for different densities. Hence the density dependency should not play a role anymore if it has only an effect on the collision time.

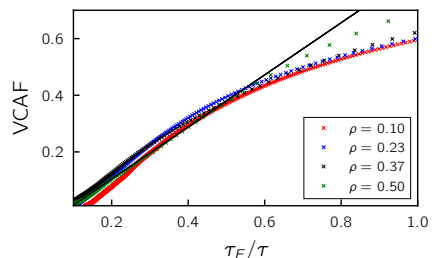


Figure 3.7 – Normalized Velocity autocorrelation function over the approximated frequency of collision.

The density dependency is not visible anymore except for very low or high collision frequency, and the VACF around the order of magnitude of the collision time is as expected comparable to  $\sim \tau^{-1}$

##### b) Calculation of Diffusion Constant

The calculation of the velocity autocorrelation function is of great interest since it can be used to calculate the diffusion constant of the system, indeed we have :



$$\begin{aligned}
 D &= \lim_{t \rightarrow \infty} \frac{1}{2t} \langle \Delta r^2(t) \rangle \\
 &= \lim_{t \rightarrow \infty} \frac{1}{2t} \int_0^t \int_0^t dt'' dt' \langle v(t'') - v(t') v(0) \rangle \\
 &= \lim_{t_1 \rightarrow \infty} \frac{1}{2t} \int_0^t dt' \int_0^t dt'' \langle v(t'') v(0) \rangle \\
 &= \lim_{t \rightarrow \infty} \frac{1}{2t} \int_{-t}^t C(\tau) d\tau \int_{\max(-\tau, t)}^{\min(2t-\tau, 2t+\tau)} dv \\
 &= \lim_{t \rightarrow \infty} \int_0^t C(\tau) \left(1 - \left|\frac{\tau}{t}\right|\right) d\tau \\
 &= \int_0^\infty C(\tau) d\tau
 \end{aligned}$$

We lead this integration explicitly since it is rarely done in the literature, we used the following change of variable :

$$\tau = t'' - t', \quad v = t'' + t'$$

The final expression is only valid when  $C(\tau)$  decays faster than  $\frac{1}{\tau}$  otherwise we got a logarithmic growth of the integral over time, this one of the numerically challenging issue when we focus on long time decay of the VACF, since we need to push the integration further, and run longer simulation. In 2d simulations we might even not be able to integrate because of the logarithmic growth of the integral. This way of calculation is commonly use but one should remember this integration subtlety. With this latter we now have three way of calculating the Diffusion coefficient, one can ask which one is the most reliable depending on the situation. M.P.Allen and D.J.Tildesley already discussed about it [CITE], and drew the following conclusions. For exponential decay of the **VCAF**, it might be more accurate to compute gradient of the **msd** rather than dividing it by the time. So we will generally prefer (3.4) than (3.5). Regarding the calculation of the diffusion constant using the autocorrelation integration, we just need to integrate over the whole time to not miss long-time contributions.

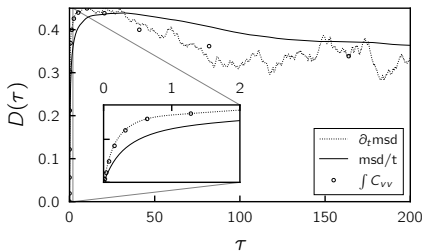


Figure 3.8 – Diffusion coefficient over time using the previous described methods

## Metropolis Algorithm

Simple sampling  
Poor Performance for Localized or Sharp Features Wasteful Computation in Low-Contribution Regions Volume of the phase space scale exponentially with the dimension.

### Why the Convergence Rate is $O(\frac{1}{\sqrt{N}})$

In Monte Carlo simulations, the estimation of an average quantity is done by sampling  $N$  independent configurations from the probability distribution of the system. The central concept underlying the convergence rate is the **law of large numbers** and the **central limit theorem**.

### Monte Carlo Estimator

Suppose we want to estimate the expected value  $\langle f \rangle$  of some function  $f(x)$ , where  $x$  is a random variable distributed according to some probability distribution  $p(x)$ . The Monte Carlo estimator for  $\langle f \rangle$  is:

$$\langle f \rangle_N = \frac{1}{N} \sum_{i=1}^N f(x_i),$$

where  $x_i$  are  $N$  independent samples drawn from  $p(x)$ .

### Variance of the Estimator

The variance of the Monte Carlo estimator is given by:

$$\text{Var}(\langle f \rangle_N) = \frac{\sigma^2}{N},$$

where  $\sigma^2$  is the variance of the function  $f(x)$  with respect to the probability distribution  $p(x)$ :

$$\sigma^2 = \langle f^2 \rangle - \langle f \rangle^2.$$

### Convergence Rate

According to the **central limit theorem**, as  $N$  increases, the distribution of  $\langle f \rangle_N$  approaches a normal distribution with mean  $\langle f \rangle$  and standard deviation  $\frac{\sigma}{\sqrt{N}}$ . This implies that the error in our estimate, which is the standard deviation of the estimator, decreases as:

$$\text{Error} \sim \frac{\sigma}{\sqrt{N}}.$$

Hence, the **convergence rate** of the Monte Carlo simulation is  $\sqrt{N}$ . This means that to reduce the error by a factor of 10, we need to increase the number of samples  $N$  by a factor of 100. This slow convergence rate is one of the limitations of simple Monte Carlo sampling.

## Implications

The  $\sqrt{N}$  convergence rate highlights why **Monte Carlo simulations** require a large number of samples to achieve high accuracy. This motivates the use of techniques like **importance sampling** and **variance reduction** to improve efficiency and obtain more accurate results with fewer samples. good sampling

### Importance Sampling in Monte Carlo Simulations

**Importance sampling** is a technique used in Monte Carlo simulations to improve the efficiency of sampling by reducing the variance of the estimator. The goal is to focus computational effort on regions of the state space that contribute most significantly to the quantity being estimated. In statistical physics, this method is crucial because the system often has many microstates with varying probabilities, and uniform sampling would be inefficient.

### Concept of Detailed Balance and Equilibrium

In statistical mechanics, **detailed balance** is a condition that ensures a system will reach and maintain equilibrium. It requires that, for any two states  $\nu$  and  $\mu$ , the rate of transitions from  $\nu$  to  $\mu$  must equal the rate of transitions from  $\mu$  to  $\nu$  at equilibrium. Mathematically, this condition is written as:

$$P(\nu)W(\nu \rightarrow \mu) = P(\mu)W(\mu \rightarrow \nu),$$

where:

- $P(\nu)$  and  $P(\mu)$  are the equilibrium probabilities of states  $\nu$  and  $\mu$ , respectively.
- $W(\nu \rightarrow \mu)$  and  $W(\mu \rightarrow \nu)$  are the transition probabilities from  $\nu$  to  $\mu$  and from  $\mu$  to  $\nu$ , respectively.

### Detailed Balance Using Flux of Random Walkers

To understand detailed balance in the context of **fluxes**, consider a collection of random walkers moving between states  $\nu$  and  $\mu$ :

- The **flux from  $\nu$  to  $\mu$**  is given by  $P(\nu)W(\nu \rightarrow \mu)$ .
- The **flux from  $\mu$  to  $\nu$**  is given by  $P(\mu)W(\mu \rightarrow \nu)$ .



At equilibrium, the net flux between  $\nu$  and  $\mu$  must be zero, implying that the fluxes are equal. This ensures that the probability distribution remains unchanged over time, maintaining a steady state.

### Applying Detailed Balance to the Ising Model

Now, consider a simple Monte Carlo scheme for simulating the Ising model:

1. Choose a random spin in the lattice.
2. Calculate the energy change  $\Delta E$  if the spin were to flip.
3. Use the following criteria to decide whether to flip the spin:
  - **Accept the flip** if  $\Delta E \leq 0$  (i.e., if the energy decreases or stays the same).
  - **Reject the flip** if  $\Delta E > 0$  (i.e., if the energy increases).

### Does This Scheme Preserve the Flux and Detailed Balance?

#### 1. Understanding the Transition Rates

- In the Ising model, the probability of transitioning from one configuration  $\nu$  to another  $\mu$  depends on the change in energy  $\Delta E$  associated with flipping a spin.
- The scheme described only accepts moves that lower or leave the energy unchanged and rejects moves that increase energy. This introduces a **bias** in the

sampling because it only allows energy-decreasing transitions, violating detailed balance.

#### 2. Violation of Detailed Balance

Since the scheme does not allow upward energy fluctuations (where  $\Delta E > 0$ ), the condition:

$$P(\nu)W(\nu \rightarrow \mu) = P(\mu)W(\mu \rightarrow \nu)$$

is not satisfied for all transitions. Thermal fluctuations are crucial for the system to explore the entire configuration space properly. By rejecting all upward transitions, the system can get trapped in local energy minima, preventing correct sampling according to the Boltzmann distribution.

#### Correcting the Scheme to Preserve Detailed Balance

To ensure that the Monte Carlo algorithm preserves detailed balance, transitions that increase energy must be allowed with appropriate probabilities. This is typically done using the **Metropolis algorithm**, where the acceptance criterion is:

- Accept the spin flip if  $\Delta E \leq 0$ .
- Accept the spin flip with probability  $\exp\left(-\frac{\Delta E}{k_B T}\right)$  if  $\Delta E > 0$ , where  $k_B$  is the Boltzmann constant and  $T$  is the temperature.

#### Why This Works

The Metropolis criterion ensures that the detailed balance condition is satisfied because:

$$\frac{W(\nu \rightarrow \mu)}{W(\mu \rightarrow \nu)} = \frac{P(\mu)}{P(\nu)} = \exp\left(-\frac{\Delta E}{k_B T}\right),$$

where  $\Delta E$  is the energy difference between states  $\nu$  and  $\mu$ . This allows the system to transition both to higher and lower energy states, maintaining the equilibrium distribution.

#### Conclusion

The proposed scheme (only accepting spin flips that lower energy) does **not preserve detailed balance** and would lead to biased sampling. Allowing transitions that increase energy with a probability given by the Boltzmann factor is essential to ensure that the system samples configurations according to the correct equilibrium distribution. This correction is crucial for accurately simulating systems like the Ising model, where fluctuations play a significant role. Importance of Ising Model explore the phase space with an importance sampling random walk.

CRTICAL SLOWING DOWN FInite size effect on first order and second order transition.

dependancy of the free energy landscape over the size (local minimum, interface ...) SECOND ORDER : the correlation length cannot diverge anymore and is limited by the system size, hence change the free energy landscape CHANGE CRITICAL EXPONENT exploit finite-size effects - don't ignore them. and can extract

FIRST ORDER : no divergence of the correlation length, metastable state and np discontinuity in the magnetization. The susceptibility is no more spiking for equilibrium state. (Have to discuss about metastable state).